

Conductivity Percolation in Loosely Compacted Microcrystalline Cellulose: An in Situ Study by Dielectric Spectroscopy during Densification

Martin Nilsson,[†] Göran Frenning,[‡] Johan Gråsjö,[‡] Göran Alderborn,[‡] and Maria Strømme^{*,†}

The Ångström Laboratory, Department of Engineering Sciences, Uppsala University, Box 534, SE 751 21 Uppsala, Sweden, and Department of Pharmacy, Uppsala Biomedical Center, Uppsala University, Box 580, SE 751 23 Uppsala, Sweden

Received: June 20, 2006; In Final Form: August 14, 2006

The present study aims at contributing to a complete understanding of the water-induced ionic charge transport in cellulose. The behavior of this transport in loosely compacted microcrystalline cellulose (MCC) powder was investigated as a function of density utilizing a new type of measurement setup, allowing for dielectric spectroscopy measurement in situ during compaction. The ionic conductivity in MCC was found to increase with increasing density until a leveling-out was observed for densities above ~ 0.7 g/cm³. Further, it was shown that the ionic conductivity vs density followed a percolation type behavior signifying the percolation of conductive paths in a 3D conducting network. The density percolation threshold was found to be between ~ 0.2 and 0.4 g/cm³, depending strongly on the cellulose moisture content. The observed percolation behavior was attributed to the forming of interparticulate bonds in the MCC and the percolation threshold dependence on moisture was linked to the moisture dependence of particle rearrangement and plastic deformation in MCC during compaction. The obtained results add to the understanding of the density-dependent water-induced ionic transport in cellulose showing that, at given moisture content, the two major parameters determining the magnitude of the conductivity are the connectedness of the interparticulate bonds and the connectedness of pores with a diameter in the 5–20 nm size range. At densities between ~ 0.7 and 1.2 g/cm³ both the bond and the pore networks have percolated, facilitating charge transport through the MCC compact.

Introduction

Already in 1960 it was shown that the ionic conductivity of compacted cellulose increases with increasing water content to the power of 9 and it was suggested that water in cellulose constituted a pathway on which alkali ions, incorporated as impurities, could move.¹ Later research put forward that also dissociated water molecules contribute to the charge transport process taking place on water molecules bound to the cellulose structure.^{2,3} Recently, it was argued that the high-exponent power-law increase in the conductivity presented by Murphy¹ was due either to a tunneling transport mechanism and/or to the strong anisotropy of the cellulose fibers.⁴ It was also shown that the behavior of the conductivity could be disassembled to a rapid increase in the number of charge carrier ions participating in the conduction process and a moderate decrease in their mobility with increasing cellulose moisture content.⁴ Furthermore, the conduction of alkali ions and/or dissociated water molecules was demonstrated to follow a percolation model⁵ with a percolation exponent of 2 and a cellulose compact porosity percolation threshold of ~ 0.1 .⁶ The critical cellulose compact pore diameter for facilitated charge transport was shown to be in the 5–20 nm range: When the network of pores with a diameter in this interval is reduced to the point where it no longer forms a continuous passageway throughout the compact, the conduction process is dominated by charge transport on the surfaces of individual microfibrils mainly situated in the bulk of fibril aggregates.

The above referred to analysis of the dependence of water-induced conductivity on pore structure and density was carried out on microcrystalline cellulose (MCC) compacts with a density above 1.0 g/cm³. The water interaction and transport properties of such tablets are of importance to, among others, the pharmaceutical sciences since MCC is one of the most frequently used excipient materials in pharmaceutical tablets. However, to get full insight into the physical parameters influencing ionic conduction in cellulose, an analysis of the low-density response must also be taken into consideration.

The aim of the present study is, thus, to analyze the behavior of water-induced charge transport in loosely compacted MCC powder as a function of density. To enable this analysis, a new type of measurement setup, allowing for dielectric spectroscopy measurement in situ during compaction, is presented and characterized.

In what follows the term “ions” refers to both the alkali ions present in the cellulose as impurities and the H_3O^+ and OH^- ions created when water molecules dissociate.

Materials and Methods

Materials. Microcrystalline cellulose (MCC; Avicel PH101) was delivered from FMC, Ireland, and used as received. Insulating pieces of close-sintered aluminum oxide (purity 99.5%) were custom-made by Keranova, Upplands Väsby, Sweden. A ceramic disk of the same material (height, 0.64 mm; purity, 96%), obtained from the same manufacturer, was used for reference measurements. A Teflon cylinder (diameter, 18.89 mm; height, 1.8 mm) was used for the same purpose.

Instrumentation. In situ dielectric spectroscopy measurements were performed by using a materials tester together with

* To whom correspondence should be addressed. Telephone: +46 18 471 72 31. E-mail: maria.stromme@angstrom.uu.se.

[†] Department of Engineering Sciences.

[‡] Uppsala Biomedical Center.

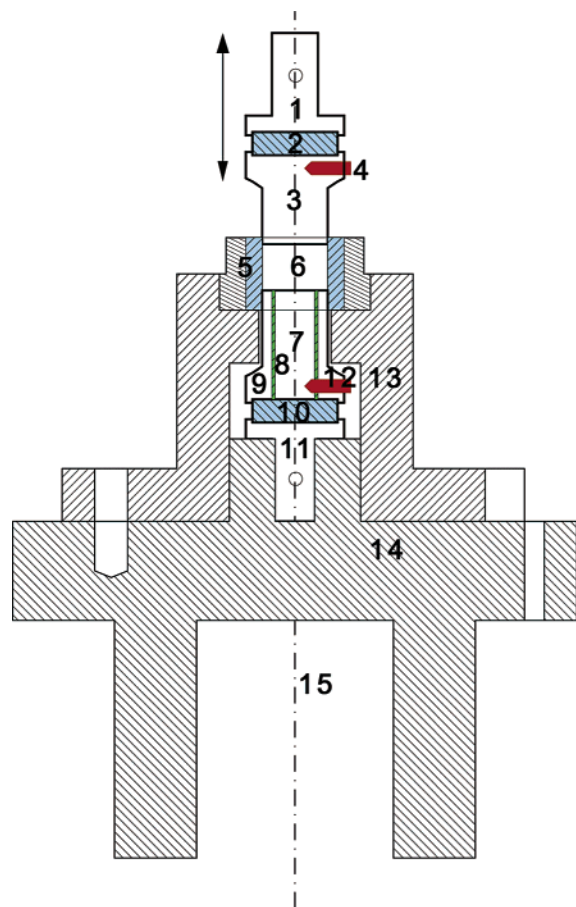


Figure 1. Schematic illustration of the dielectric measurement system, showing the punches, the die, and two steel parts (13 and 14) used to attach the die and the lower punch to the lower grip of the materials tester (15). The upper punch consists of a mounting part (1), an insulating ceramic disk (2), an electrode (3), and a contact (4). The die (5) consists of an outer steel part and an inner ceramic part that enclose the die cavity (6). The lower punch consists of an inner measurement electrode (7), separated by a Teflon layer (8) from the guard (9), an insulating ceramic disk (10), a mounting part (11), and a contact (12).

a dielectric spectroscopy instrument. The materials tester used was a Zwick Z100 (Zwick/Roell, Zwick GmbH & Co. KG, Germany) equipped with a 100 kN load cell. A Novocontrol Alpha-AN high-performance frequency analyzer and a ZG2 2-wire test interface (Novocontrol Technologies GmbH & Co. KG, Hundsangen, Germany) constituted the dielectric instrument. A flat-faced stationary lower punch (diameter, 18.89 mm) and a die were mounted on the lower grip, and a mobile upper punch on the load cell, which itself was mounted on the crosshead of the materials tester. All distance readings were corrected for deformations of the mechanical system by using a predetermined correction curve.

The punches and die were specially designed to allow accurate in situ dielectric spectroscopy measurements to be performed during compaction. The upper punch consisted of two stainless steel parts, one of which constituted the electrode, and the other the mounting part. These two parts are electrically insulated from each other by a ceramic disk (7.0 mm high and 26.5 mm in diameter) as shown in Figure 1. The lower punch was designed in a similar manner, but the electrode, in turn, was separated into two different concentric parts by a 1.0 mm thick Teflon layer, to produce an inner measurement electrode and an outer guard. The guard was maintained at the same potential as the measurement electrode but was not part of the actual measurement system. The purpose of the guard was to

reduce edge effects by restricting the measurement to the central part of the die cavity, where the electric field is more uniform. The measurement electrode arrangement (the central electrode of the lower punch and corresponding area of the upper punch electrode) could thus be regarded as a parallel plate capacitor, with known empty space capacitance.

The die consisted of an inner hollow insulating cylinder, made from the above-described ceramic material (height, 22 mm; inner diameter, 18.89 mm; outer diameter, 25 mm), and an outer stainless steel part, as illustrated in Figure 1. The upper face of the lower punch was located approximately 5 mm above the bottom of the die, thus leaving 17 mm for the powder material to be analyzed.

Dielectric Spectroscopy Characterization of the Experimental Setup. A number of tests were performed in order to characterize the performance of the dielectric measurement system. First, the dielectric response of the 96% pure close-sintered aluminum oxide disk was determined by using a standard setup described elsewhere.⁷ Second, the performances of the punches and die were evaluated by using a custom-made cylindrical Teflon sample with known dielectric response. Third, measurements were performed on the empty die cavity, for a series of punch-to-punch distances.

In Situ Dielectric Spectroscopy Measurements. Prior to the dielectric spectroscopy measurements, the MCC powder was conditioned by first storing it in a desiccator over P_2O_5 and then letting it equilibrate in the humid laboratory environment for at least 5 days. The relative humidity (RH) in the laboratory was continuously monitored, and the variation in RH in the 5 day period prior to—and during—a measurement never exceeded 1%. All measurements were performed at room temperature.

For each measurement series, the desired amount of MCC powder (~100–200 mg, corresponding to a compact thickness between ~0.90 and 2.00 mm) was carefully weighed and poured into the die cavity. The upper punch was lowered to a pre-selected position and then held fixed at that position. Once the measured force was considered stationary, the dielectric spectroscopy measurement was started. A sinusoidal voltage of amplitude 3.0 V was applied across the sample, and the frequency was swept from 1 MHz down to 10 mHz.

The measurements were performed as several series of a sequence of decreasing punch-to-punch distances on a MCC sample and the dielectric response was assessed as a function of the bulk density of the powder and the RH at which the powder had been stored and measured.

Results and Discussions

Verification of the Experimental Setup. Figure 2a shows the real part of the dielectric permittivity (ϵ') for the 0.64 mm high and 96% pure close-sintered aluminum oxide disk. Close-sintered aluminum oxide was selected as insulating material in the dielectric measurement system because of its high mechanical strength and flat dielectric response. That this material indeed exhibits a flat response, with very little dispersion for frequencies between 10^{-2} and 10^6 Hz and a ϵ' value of ~9.33, is evident from the figure. The relative dielectric permittivity for aluminum oxide has earlier been reported to lie in the 9.3–12.0 interval.^{8,9}

Figure 2a also shows the real part of the dielectric permittivity of the 1.8 mm high Teflon cylinder, determined by using the newly developed dielectric measurement system. Again a flat dielectric response is seen, with a relative dielectric permittivity of ~2.08 that compares favorably with literature values which are between 2.0 and 2.2. Teflon was used as insulating material

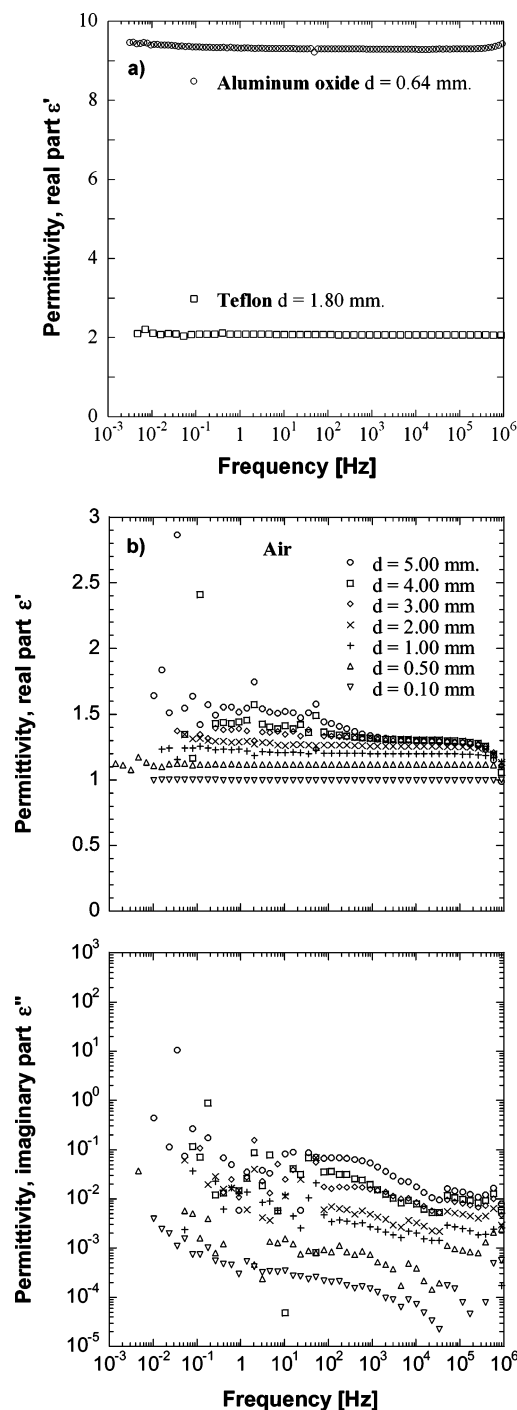


Figure 2. (a) Real part of the permittivity for the 96% pure close-sintered aluminum oxide disk, determined utilizing a setup with a guard, and of the Teflon cylinder, determined by using the newly developed dielectric measurement system. (b) Dielectric response of the dielectric measurement system, with an air-filled die cavity, for a number of punch-to-punch distances.

between the inner measurement electrode and outer guard of the lower punch because of its ability to deform without cracking and its flat dielectric response.

Figure 2b shows the dielectric response of the newly developed dielectric measurement system for an empty (i.e., air-filled) die cavity and a number of punch-to-punch distances. With decreasing punch-to-punch distance, the real part of the permittivity is seen to approach a value of unity and to be virtually independent of frequency, as expected for a die cavity filled with air. For punch-to-punch distances exceeding 0.5–1 mm,

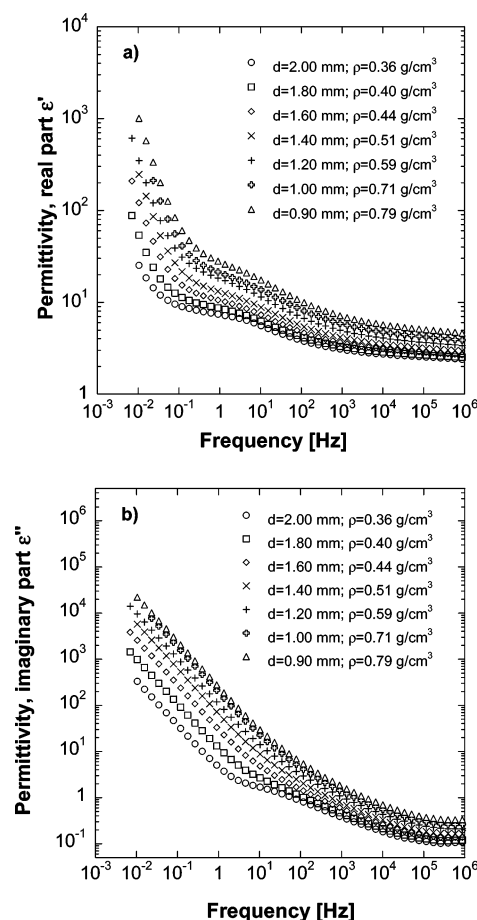


Figure 3. Real (a) and imaginary (b) part of the permittivity for MCC equilibrated at an RH of 60%. The MCC powder mass was kept constant, 200.4 mg, and the punch distances diminished during the measurements. The punch separation, d , and the inherent MCC bulk density, ρ , are also displayed.

the measured permittivity inevitably has a small contribution from imperfections of the measurement system, e.g., capacitive coupling between cables and capacitive coupling between electrodes and other metallic parts of the materials tester. The imaginary part of the permittivity is seen to be much lower than 1 for all frequencies when the electrode separation is smaller than ~ 3 mm and for the high-frequency part of the spectrum at larger electrode separations, signifying a response with very limited frequency dispersion. To ensure reliable dielectric spectroscopy results when measuring on the MCC powder, the electrode separation is kept below 3 mm.

Permittivity Spectra. Figure 3 shows a sequence of dielectric permittivity data of MCC equilibrated and recorded at an RH of 60% for decreasing punch separations and, thus, for increasing cellulose densities. From the figure it is obvious that both the real (ϵ') and the imaginary (ϵ'') parts of the permittivity increase during densification. In the ϵ'' spectra a dipolar loss process, the so-called β_{wet} relaxation associated with the collective motions of a water–cellulose mixed phase,^{10–12} is visible at ~ 10 – 100 Hz for the lowest density compact. At higher densities dc-like imperfect charge transport,^{13,14} giving rise to the power-law increase¹⁵ observed in ϵ'' toward lower frequencies, dominates the spectra. However, the presence of the β_{wet} relaxation also for the more densely packed powder is evident from the steps visible in all recorded ϵ' spectra in the 10–100 Hz region. Permittivity spectra recorded at lower RHs show behavior similar to those measured at 60% RH. However, the onset of the β_{wet} relaxation process and the dc-like imperfect charge

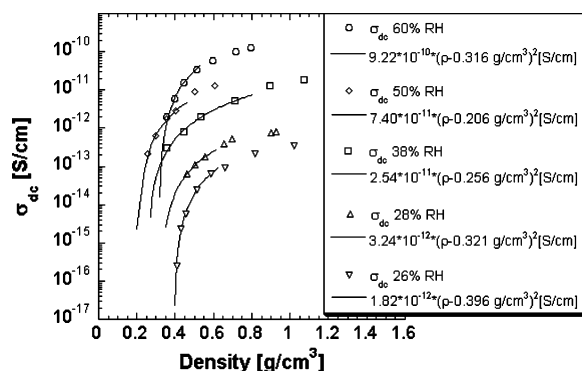


Figure 4. Selected conductivity values, σ_{dc} , obtained for five different RHs during MCC powder densification. The initial parts of the conductivity vs density curves are fitted to eq 1 and shown as solid lines. The equations describing the fits are also displayed.

transport process are shifted toward lower frequencies with decreasing RH, as reported earlier.¹⁶

Density Dependence of Conductivity. Figure 4 shows five sets of conductivity values, pertaining to different RHs, extracted from the dc-like imperfect charge transport region of permittivity spectra similar to those in Figure 3 using the method outlined in refs 4, 17, and 18. The conductivity clearly increases with increasing density until a leveling-out is observed for densities above ~ 0.7 g/cm³. In earlier measurements on high-density MCC,¹³ the conductivity was found to decrease with increasing density from a plateau value at slightly above 1 g/cm³. As explained above, this decrease could later be linked to the disappearance of a connected network of pores with diameters between ~ 5 and 20 nm as densification proceeded beyond ~ 1.2 g/cm³.⁶ Through an analysis of the conductivity curves, of which some examples are shown in Figure 4, it was found that they followed a power-law behavior with an exponent of 2 according to

$$\sigma_{dc}(\rho) = \sigma_0(\rho - \rho_c)^2 \quad (1)$$

at low densities. Here σ_0 is a constant independent of density and ρ_c denotes the density value above which the MCC starts to conduct ions. Fits to eq 1 are included in Figure 4. According to percolation theory, the above equation describes percolation of conductive paths in a 3D conducting network.⁵

Percolation expressions of the type shown in eq 1 have been shown to describe conduction processes for densities lower than ~ 0.2 – 0.3 above ρ_c in relative measures. Above this region effective medium theory usually describes a conduction process.¹⁹ Since the true density of MCC is ~ 1.6 g/cm³,^{20–22} eq 1 is not expected to describe the conduction mechanisms for densities above $\rho_c + \sim (0.32$ – $0.48)$ g/cm³. Curve fits of the type shown in Figure 4 were thus produced below this upper density limit.

From fits similar to those in Figure 4, the density percolation threshold ρ_c could be extracted. These threshold values are shown as a function of RH in Figure 5. It is evident that the percolation threshold decreases with increasing RH for RH values below $\sim 50\%$. At the highest RH of this study, 60%, an increase in ρ_c is detected.

The fact that the conductivity, associated with water-induced ionic charge transport in MCC, clearly follows a percolation behavior at low densities can only be explained by the successive creation of conductivity pathways as densification proceeds. For MCC, which consolidates mainly by plastic deformation, compaction may be described in terms of three dominant pro-

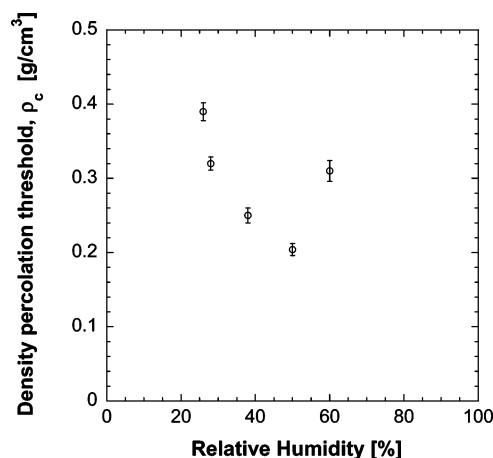


Figure 5. Density percolation threshold ρ_c —extracted from fits similar to those in Figure 4 and associated with water-induced ionic transport in MCC—vs MCC equilibration RH. The error bars signify standard deviations for three measurements.

cesses: Particle rearrangement, plastic deformation of particles, and formation of interparticulate bonds.²³ For other materials particle fragmentation and elastic deformation of particles may be of importance as well. Moreover, powder compaction is often considered to occur in sequential stages, where each stage is represented by the mechanism that dominates or controls the process in that stage. It has been suggested that a stage dominated by particle rearrangement and fragmentation is followed by a stage dominated by elastic/plastic particle deformation,²⁴ while the extent of interparticulate bonding gradually increases. It has further been suggested that at MCC moisture contents below ~ 5 wt % (representing a RH $\sim 50\%$) most sorbed water molecules are hydrogen-bonded within MCC particles,^{25,26} leaving no or very few molecules available to form a bulk water phase that can moisturize the environment between adjacent particles. Thus, the onset of the water-induced ionic transport in MCC, characterized by eq 1, most likely coincides with the forming of the interparticulate bonds since a measurable ionic transport requires a continuous pathway for the ions to move also between particles.

The lowering of the density percolation threshold with increasing RH, observed in Figure 5 at RHs below $\sim 50\%$, may be explained by a combination of two factors: An increased plastic deformation propensity and a decreased tendency for particle rearrangement. Earlier experience shows that the presence of 5 wt % water may reduce the yield pressure determined from a Heckel analysis by as much as 25% compared to the dry state.²⁷ Moreover, it appears to be a general consensus that water reduces the flowability of MCC powder, as indicated for instance by shear cell experiments.²⁸ Hence, with increasing moisture contents in the powder, a jammed state²⁹ is reached and interparticulate bonds with comparatively large bonding surfaces are formed earlier in the compaction process, thus promoting the formation of a bond-percolation cluster that spans through the entire powder bed at successively lower densities with increasing moisture contents.

Presently we have no solid explanation for the observed increase in the percolation threshold value observed at 60% RH, corresponding to a cellulose moisture content of ~ 6 wt %.⁴ However, it is remarkable that this increase coincides with the moisture content interval for which a bulk water phase in the cellulose starts to form.²⁵ At these high moisture contents capillary condensation, instead of multilayer adsorption, starts to dominate the water adsorption process in the material.³⁰ As

well, the behavior of the ionic conduction has been shown to change nature, most likely due to swelling in the cellulose fiber structure.³

After an unbroken bond-percolation cluster—extending through the entire MCC compact—has been formed, the conductivity clearly continues to increase until the observed leveling-out is detected for densities above ~ 0.7 g/cm³, Figure 4. From the above-mentioned earlier findings⁶ that this leveling-out is discontinued and a region of conductivity decrease with increasing density is observed—as a consequence of the disappearance of a continuous network of mesopores—a full picture of the density dependence of the ionic transport in cellulose can be assembled. At a given moisture content there are apparently two parameters determining the magnitude of the water-induced ionic conductivity in MCC: The connectedness of the interparticulate bonds and the connectedness of pores with a diameter in the 5–20 nm size range. At densities between ~ 0.7 and 1.2 g/cm³ both the bond and the pore networks have percolated, paving the way for a facilitated charge transport through the MCC compact.

Summary and Conclusion

The behavior of water-induced charge transport in loosely compacted MCC powder was investigated as a function of density, employing a new type of measurement setup, allowing for dielectric spectroscopy measurement in situ during compaction. The setup was characterized dielectrically and verified to give reliable results for the dielectric response of the material tested as long as the thickness of the powder bed was below ~ 3 mm.

The ionic conductivity in MCC was found to increase with increasing density until a leveling-out was observed for densities above ~ 0.7 g/cm³. Furthermore, it was found that the conductivity vs density followed a percolation type behavior with a percolation exponent of 2 and a density percolation threshold between ~ 0.2 and 0.4 g/cm³, depending strongly on the cellulose moisture content. The observed percolation behavior was attributed to the forming of interparticulate bonds in the MCC powder bed, whereas the percolation threshold dependence on moisture was linked to the moisture dependence of particle rearrangement and plastic deformation in the MCC compaction process.

The presented results add to the complete understanding of the density dependent water-induced ionic transport in cellulose, showing that at a given moisture content there are two major parameters determining the magnitude of the conductivity: The connectedness of the interparticulate bonds and, as earlier put forward,⁶ the connectedness of pores with a diameter in the 5–20 nm size range. At densities between ~ 0.7 and 1.2 g/cm³ both the bond and the pore networks have percolated, paving the way for a facilitated charge transport through the MCC compact.

Acknowledgment. M.S. is a Royal Swedish Academy of Sciences (KVA) Research Fellow and would like to thank the Academy for their support. The Knut and Alice Wallenberg Foundation is acknowledged for their financial support to the new setup employed. The Swedish Foundation for Strategic Research (SSF) is also acknowledged for their support to our multidisciplinary research in materials physics and pharmaceuticals.

References and Notes

- (1) Murphy, E. J. *J. Phys. Chem. Solids* **1960**, *16*, 115.
- (2) Pethig, R. *Dielectric and Electronic Properties of Biological Materials*; Wiley: Chichester, U.K., 1979.
- (3) Sapieha, S.; Inoue, M.; Lepoutre, P. *J. Appl. Polym. Sci.* **1985**, *30*, 1257.
- (4) Nilsson, M.; Strømme, M. *J. Phys. Chem. B* **2005**, *109*, 5450.
- (5) Sahimi, M. *Applications of Percolation Theory*; Taylor & Francis: London, U.K., 1994.
- (6) Nilsson, M.; Mhrranyan, A.; Valizadeh, S.; Strømme, M. *J. Phys. Chem. B* **2006**, *110*, 15776.
- (7) Hägerström, H.; Edsman, K.; Strømme, M. *J. Pharm. Sci.* **2003**, *92*, 1869.
- (8) Lide, D. R. *CRC Handbook of Chemistry and Physics*, 73 ed.; CRC Press: Boca Raton, FL, 1992.
- (9) Samsonov, G. V. *The Oxide Handbook*, 2nd ed.; IFI/Plenum: New York, 1982.
- (10) Einfeldt, J.; Meissner, D.; Kwasniewski, A. *Macromol. Chem. Phys.* **2000**, *201*, 1969.
- (11) Einfeldt, J.; Meissner, D.; Kwasniewski, A.; Einfeldt, L. *Polymer* **2001**, *42*, 7049.
- (12) Einfeldt, J.; Kwasniewski, A. *Cellulose* **2002**, *9*, 225.
- (13) Nilsson, M.; Alderborn, G.; Strømme, M. *Chem. Phys.* **2003**, *295*, 159.
- (14) Hill, R. M.; Dissado, L. A. *Solid State Ionics* **1988**, *26*, 295.
- (15) Jonscher, A. K. *Dielectric Relaxations in Solids*; Chelsea Dielectric Press: London, 1983.
- (16) Ek, R.; Hill, R. M.; Newton, J. M. *J. Mater. Sci.* **1997**, *32*, 4807.
- (17) Strømme-Mattsson, M.; Niklasson, G. A. *J. Appl. Phys.* **1999**, *85*, 8199.
- (18) Niklasson, G. A.; Jonsson, A. K.; Strømme, M. Impedance Response of Electrochromic Materials and Devices. In *Impedance Spectroscopy*, 2nd ed.; Barsoukov, Y., Macdonald, J. R., Eds.; Wiley: New York, 2005.
- (19) Kirkpatrick, S. *Rev. Mod. Phys.* **1973**, *45*, 574.
- (20) Gustafsson, C.; Lennholm, H.; Iversen, T.; Nyström, C. *Drug Dev. Ind. Pharm.* **2003**, *29*, 1095.
- (21) Zhang, Y.; Law, Y.; Chakrabarti, S. *AAPS Pharm. Sci. Technol.* **2003**, *4*, article 62.
- (22) Schmidt, C.; Leinebudde, P. K. *Chem. Pharm. Bull.* **1999**, *47*, 405.
- (23) Nyström, C.; Karehill, P.-G. *The Importance of Intermolecular Bonding Forces and the Concept of Bonding Surface Area*; Dekker: New York, 1996.
- (24) Duberg, M.; Nyström, C. *Powder Technol.* **1986**, *46*, 67.
- (25) Khan, F.; Pilpel, N. *Powder Technol.* **1987**, *50*, 237.
- (26) Bolhuis, G. K.; Chowan, Z. T. *Materials for Direct Compaction*; Dekker: New York, 1996.
- (27) Khan, F.; Pilpel, N.; Ingham, S. *Powder Technol.* **1988**, *54*, 161.
- (28) Amidon, G. E.; Houghton, M. E. *Pharm. Res.* **1995**, *12*, 923–929.
- (29) Cates, M. E.; Wittmer, J. P.; Bouchaud, J.-P.; Claudin, P. *Phys. Rev. Lett.* **1998**, *81*, 1841.
- (30) Mhrranyan, A.; Strømme, M. *Chem. Phys. Lett.* **2004**, *393*, 389.